

**CHEM****MED****CHEM**  
Chemistry &  
Drug Discovery

## Supporting Information

© Copyright Wiley-VCH Verlag GmbH & Co. KGaA, 69451 Weinheim, 2009

# Aryldiketo Acids Have Antibacterial Activity Against MDR *S. aureus* Strains. The Structural Insight Based on Similarity and Molecular Interaction Fields.

Branko J. Drakulić, Michal Stavri, Simon Gibbons, Željko S. Žižak, Tatjana Ž. Verbić, Ivan O. Juranić, Mire Zloh

## Table of Contents of Supplementary Information

List of Tables .....	2
List of figures.....	2
Experimental Section:.....	3
Materials .....	3
Synthetic procedure .....	3
<b>8</b> 4-(2,4-diisopropylphenyl)-2,4-dioxo-2-butenoic acid: .....	4
<b>9</b> 4-(2,5-diisopropylphenyl)-2,4-dioxo-2-butenoic acid: .....	4
<b>10</b> 4-(2,4,6-triethylphenyl)-2,4-dioxo-2-butenoic acid:.....	4
<b>11</b> 4-(2,4,6-triisopropylphenyl)-2,4-dioxo-2-butenoic acid: .....	5
<b>12</b> 4-biphenyl-4-yl-2,4-dioxo-2-butenoic acid: .....	5
<b>20</b> 4-(1 <i>H</i> -Indol-3-yl)-2,4-dioxo-2-butenoic acid: .....	5
Antibacterial assay: .....	6
Cytotoxicity assays: .....	6
Preparation of drugs solution:.....	6
Preparation of peripheral blood mononuclear cells (PBMC): .....	7
Treatment of PBMC from normal healthy donors:.....	7
Determination of PBMC survival:.....	7
<i>Calculation protocols:</i> .....	8
<i>Building ALMOND models:</i> .....	8
Supporting Results and Discussion .....	10
Cytotoxicity results.....	10
Almond Model.....	11
Comparative analysis of ALMOND models related to neutral and ionized forms of molecules.....	17
References.....	23

## List of Tables

Table 1S. Cytotoxicity, expressed as IC <sub>50</sub> and IC <sub>90</sub> (concentration that inhibit 50% and 90% growth, respectively), of selected compounds toward healthy human cells PBMC (peripheral blood mononuclear cells) non-stimulated and stimulated for proliferation with phytohaemagglutinin (PHA)..	10
Table 2S. Statistics of PLS model for neutral forms of <b>5, 8 - 10, 12, 15, 17, 19, 21-24</b> . ....	11
Table 3S. Statistics of PLS model for ionised forms of <b>5, 8 - 10, 12, 15, 17, 19, 21-24</b> ....	11
Table 4S. Variables having high impact on the model related to neutral forms of <b>5, 8 -10, 12, 15, 17, 19, and 21 - 24</b> . ....	12
Table 5S. Variables having high impact on the model related to ionized forms of <b>5, 8 - 10, 12, 15, 17, 19 and 21 - 24</b> . ....	13
Table 6S. Presence of variables associated with compounds, in the model for neutral forms of <b>5, 8 - 10, 12, 15, 17, 19 and 21 - 24</b> . ....	14
Table 7S. Presence of variables associated with compounds, in the model for ionized forms of <b>5, 8 - 10, 12, 15, 17, 19 and 21 - 24</b> . ....	14
Table 8S. Observed vs. Calculated log (1/MIC) against SA-1199B for <b>5, 8 - 10, 12, 15, 17, 19, 21 - 24</b> in their molecular and ionized forms. MIC is in mol/L. ....	15
Table 9S. GRID MG+2 probe minima for compounds <b>5, 8 - 10, 12, 15, 17, 19, 21 - 24</b> in their ionization states under the physiological pH (7.35). ....	16
Table 10S. Interaction energies between ADKs and norfloxacin calculated by Glue without (w/o) and with (w) electrostatic contribution using procedure described previously. <sup>18</sup> .....	16

## List of figures

Scheme 1S. Structures of commercial antibiotics ( <b>21-24</b> ) used in ALMOND models....	18
Panel IS. ....	19
Panel IIS. ....	20
<b>Figure 1S.</b> MG+2 GRID probe isocountour levels for <b>8, 9, 12, 22 and 23</b> , in their ionized forms on physiological pH (7.35).....	22

## Experimental Section:

### Materials

All chemical used were purchased from Fluka or Aldrich, having > 98% purity. Melting points were taken on Büchi apparatus in open capillary tubes and were uncorrected. The NMR spectra were acquired using Bruker Avance 500/125 MHz NMR instrument. Samples for NMR characterization were dissolved in DMSO- $d_6$  and spectra calibrated using residual solvent signals ( $\delta$  DMSO- $d_6$ :  $^1\text{H}$ : 2.50 ppm,  $^{13}\text{C}$  39.70 ppm;). Mass spectra (LC HR/ESI-MS) were recorded on Agilent Technologies 6210 TOF LC ESI-MS instrument in positive or negative mode, using MeOH as a solvent. IR spectra were taken on Thermo-Nicolet 6700 FT-IR spectrometer (ATR) Combustion analyses were done on Vario EL III, CHNS Elemental Analyzer (Elementar). All reported compounds (**1-20**) are confirming >98 % purity, based on combustion analysis data.

### Synthetic procedure

Synthesis and characterization of **1-7**, **13-19** was described previously.<sup>1,2</sup> The same samples were used for antibacterial and cytotoxicity assays. Synthesis of **9-12**, **20**: For synthesis of **12** and **20**, commercially available acetophenones were used. For synthesis of **8-11**, the commercially available alkylbenzenes (1,3-di-*i*-Pr-benzene, 1,4-di-*i*-Pr-benzene, 1,3,5-tri-Et-benzene and 1,3,5-tri-*i*-Pr-benzene for **8-11**, respectively) were used. Acylation with AcCl in  $\text{CH}_2\text{Cl}_2$ , using  $\text{AlCl}_3$  as a catalyst, under cooling, afforded corresponding acetophenones, which were purified by distillation under reduced pressure (crystallization for 2,4,6-tri-*i*-Pr-acetophenone (PhH)) and characterized by  $^1\text{H}$  and  $^{13}\text{C}$  NMR spectroscopy. Pure acetophenones were used for condensation with diethyloxalate (1:1) in presence of 2 molar equivalents of NaOMe (obtained by dissolution of Na in dry MeOH) during 16-18 h. The reaction mixture was quenched by ice-cold acidified water (HCl, pH = 2-3) and stirred 4-5 h. Et-ester of **12** was hydrolyzed using dioxane/1M NaOH (1:1) during 3h and the crude product purified by crystallization. Other crude products were extracted with di-*i*-Pr ether, organic layer thoroughly washed with water, dried

with anhydrous CaSO<sub>4</sub> and concentrated under reduced pressure. Pure products were obtained by crystallization. pK<sub>a</sub> value of **8-10** were determined using the same procedures as described previously.<sup>1,2</sup>

**8** *4-(2,4-diisopropylphenyl)-2,4-dioxo-2-butenoic acid:*

Light yellow crystals, C<sub>16</sub>H<sub>20</sub>O<sub>4</sub>; ESI-MS HR (solvent MeOH, positive mode): 277.1442 [M+H]<sup>+</sup> (Calc. Mass 276.1362). Melting point 124-126 °C ((*i*-Pr)<sub>2</sub>O). IR  $\nu$  (cm<sup>-1</sup>): 1713.4, 1622.5, 1608.4, 1397.1, 1276.5. <sup>1</sup>H NMR 500 MHz (DMSO-*d*<sub>6</sub>, 27 °C),  $\delta$  (ppm): ~ 14 (*b*), 7.465 (*d*, 1H, *J* = 8.22 Hz), 7.351 (*d*, 1H, *J* = 1.19 Hz), 7.212 (*dd*, 1H, *J*<sub>1,2</sub> = 1.71 Hz, *J*<sub>1,3</sub> = 7.90 Hz), 6.61 (*s*, integral 0.13, correspond to 2H from diketo tautomer), 2.43 (*h*, 1H, *J* = 7.07 Hz, merged with diketo heptet), 2.937 (*h*, 1H, *J* = 7.15 Hz), 1.215 (*d*, 6H, *J* = 2.93 Hz), 1.995 (*d*, 6H, *J* = 2.44 Hz). <sup>13</sup>C NMR 125 MHz (DMSO-*d*<sub>6</sub>, 27 °C),  $\delta$  (ppm): 196.17, 167.75, 163.36, 152.63, 148.15, 133.78, 128.84, 124.81, 123.90, 102.54, 33.77, 29.18, 24.19, 23.74.

**9** *4-(2,5-diisopropylphenyl)-2,4-dioxo-2-butenoic acid:*

Light yellow semisolid, C<sub>16</sub>H<sub>20</sub>O<sub>4</sub>; ESI-MS HR (solvent MeOH, positive mode): 277.1440 [M+H]<sup>+</sup> (Calc. Mass 276.1362); Melting point 124-126 °C ((*i*-Pr)<sub>2</sub>O). IR  $\nu$  (cm<sup>-1</sup>): 1721.2, 1631.9, 1617.9, 1588.3, 1439.5, 1263.0. <sup>1</sup>H NMR 500 MHz (DMSO-*d*<sub>6</sub>, 27 °C),  $\delta$  (ppm): 6.563, (*s*, 1H), 4.482, (*s*, 2H, intensity 0.16 in respect to enol H3 – diketo tautomer), 3.230 (*s*, *b*, 1H), 2.923 (*s*, 1H), 1.204 (*d*, 2H), 1.187 (*d*, 6H), <sup>13</sup>C NMR 125 MHz (DMSO-*d*<sub>6</sub>, 27 °C),  $\delta$  (ppm): 196.21, 168.21, 163.36, 146.19, 144.84, 136.21, 129.87, 126.89, 125.86, 102.65, 33.02, 28.09, 24.22, 23.86.

**10** *4-(2,4,6-triethylphenyl)-2,4-dioxo-2-butenoic acid:*

Light yellow crystals, C<sub>16</sub>H<sub>20</sub>O<sub>4</sub>; ESI-MS HR (solvent MeOH, positive mode): 277.14344 [M+H]<sup>+</sup>, (Calc. Mass 276.13616); 189.1266, 34.45 %). Melting point 124-125 °C (Hexane). IR  $\nu$  (cm<sup>-1</sup>): 1711.7, 1624.2, 1603.5, 1584.7, 1399.0, 1274.0. <sup>1</sup>H NMR 500 MHz (DMSO-*d*<sub>6</sub>, 27 °C),  $\delta$  (ppm): 6.99 (*s*, 3H), 6.26 (*s*, *b* ~ 1H), 4.28 (*s*, low intensity from diketo tautomer), 2.59 (*q*, *J*<sub>1,2</sub> = 7.63 Hz, *J*<sub>1,3</sub> = 15.26 Hz, 2H), ~ 2.59 (*q*, overlapped with DMSO-*d*<sub>6</sub> signals), 1.19 (*t*, *J* = 7.63 Hz, 3H), 1.11 (*t*, *J* = 7.63 Hz, 6H). <sup>13</sup>C

NMR 125 MHz (DMSO-*d*<sub>6</sub>, 27 °C),  $\delta$  (ppm): 195.49, 168.89, 163.37, 145.16, 139.86, 134.77, 125.54, 113.84, 27.92, 25.74, 15.79, 15.24.

**11 4-(2,4,6-triisopropylphenyl)-2,4-dioxo-2-butenoic acid:**

Light yellow crystals, C<sub>16</sub>H<sub>20</sub>O<sub>4</sub>; ESI-MS HR (solvent MeOH, negative mode): 317.1757 [M-H], (Calc. Mass 318.1831). Melting point 76-78 °C (PhH). Unstable for full characterization.

(2,4,6-Triisopropylphenyl)-ethan-1-one. Colorless crystals (EtOH/H<sub>2</sub>O). IR  $\nu$  (cm<sup>-1</sup>): 1691.1, 1457.1, 1357.5, 1240.4. <sup>1</sup>H NMR 200 MHz (DMSO-*d*<sub>6</sub>, 25 °C),  $\delta$  (ppm): 7.049 (*s*, 2H), 2.867 (*h*, 1H, *J* = 6.74 Hz), 2.626 (*h*, 2H, 6.73 Hz), 2.440 (*s*, 3H), 1.182 (*m*, 18 H). <sup>13</sup>C NMR 50 MHz (DMSO-*d*<sub>6</sub>, 25 °C),  $\delta$  (ppm): 208.815, 149.184, 142.830, 138.569, 120.998, 33.837, 33.760, 30.578, 24.278, 24.059.

**12 4-biphenyl-4-yl-2,4-dioxo-2-butenoic acid:**

White solid, C<sub>16</sub>H<sub>12</sub>O<sub>4</sub>; ESI-MS HR (solvent MeOH, positive mode): 269.0819 [M+H]<sup>+</sup> (Calc. Mass 268.0736); Melting point 125-128 °C (AcOEt). IR  $\nu$  (cm<sup>-1</sup>): 1711.0, 1630.0, 1591.0, 1406.0, 1274.0. <sup>1</sup>H NMR 500 MHz (DMSO-*d*<sub>6</sub>, 27 °C),  $\delta$  (ppm): 13.99 (*b*), 8.13 (*d*, 2H, *J* = 8.98 Hz), 7.85 (*d*, 2H, *J* = 8.23 Hz), 7.75 (*d*, 2H, *J* = 7.76 Hz), 7.50 (*t*, 2H, *J* = 7.94 Hz), 7.43 (*l*, 1H, *J* = 7.68 Hz), 7.14 (*s*, 1H), 4.60 (*s*, 2H, intensity 0.16 in respect to enol H3 – diketo tautomer). <sup>13</sup>C NMR 125 MHz (DMSO-*d*<sub>6</sub>, 27 °C),  $\delta$  (ppm): 189.89, 170.45, 163.35, 145.51, 138.81, 133.57, 129.31, 128.79, 127.20, 98.05.

**20 4-(1H-Indol-3-yl)-2,4-dioxo-2-butenoic acid:**

Orange-yellow solid, C<sub>12</sub>H<sub>9</sub>NO<sub>4</sub> ESI-MS HR (solvent MeOH, negative mode): 230.0455 [M-H] (Calc. Mass 231.0532); Melting point 205-208 °C (AcOEt). IR  $\nu$  (cm<sup>-1</sup>): 1613.1, 1576.2, 1525.1, 1440.0, 1258.4. <sup>1</sup>H NMR 500 MHz (DMSO-*d*<sub>6</sub>, 27 °C),  $\delta$  (ppm): 12.44 (*s, b*, 1H), 8.75 (*d*, *J* = 3.19 Hz, 1H), 8.28 (*d*, *J* = 1.79 Hz, 1H), 7.57 (*d*, *J* = 6.83 Hz, 1H), 7.32 (*t*, *J* = 7.25 Hz, 2H), 7.01 (*s*, 1H), 4.41 (*b*), from diketo tautomer. <sup>13</sup>C NMR 125 MHz (DMSO-*d*<sub>6</sub>, 27 °C),  $\delta$  (ppm): 192.87, 189.68, 164.03, 137.32, 135.90, 125.38, 116.93, 116.03, 122.60, 121.75, 112.82, 100.56, 52.97 (from diketo tautomer).

### **Antibacterial assay:**

*S. aureus* strain ATCC 25923 was the generous gift of E. Udo (Kuwait University, Kuwait). *S. aureus* RN4220 containing plasmid pUL5054, which carries the gene encoding the MsrA macrolide efflux protein, was provided by J. Cove.<sup>3</sup> Strains XU212 and IS-58, which possesses the TetK tetracycline efflux protein, were provided by E. Udo.<sup>4</sup> Strain CD1281 which possesses the TetK tetracycline efflux protein was provided by C. Dowson. SA-1199B, which overexpresses the *norA* gene encoding the NorA MDR efflux protein was provided by G. Kaatz.<sup>5</sup> Strain EMRSA-15 was provided by P. Stapleton. All *Staphylococcus aureus* strains were cultured on nutrient agar and incubated for 24 h at 37 °C prior to MIC determination. Bacterial inocula equivalent to the 0.5 McFarland turbidity standard were prepared in normal saline and diluted to give a final inoculum density of  $5 \times 10^5$  cfu/ml. The inoculum (125  $\mu$ l) was added to all wells, and the microtitre plate was incubated at 37 °C for 18 h. The MIC was recorded as the lowest concentration at which no bacterial growth was observed as previously described.<sup>5</sup> The potentiating effect of these compounds was determined by dissolving in DMSO before diluting into MHB for use in the MIC determinations. Norfloxacin, erythromycin and tetracycline were purchased from Sigma-Aldrich and used for antibacterial assays without further purifications (purity >95%).

### **Cytotoxicity assays:**

#### *Preparation of drugs solution:*

Stock solutions of the investigated compounds were made in dimethylsulfoxide (Fluka Chemie AG Buchs, Switzerland) at a concentration of 20 mM, filtered through Millipore filter (0.22  $\mu$ M), before use, and afterwards diluted to various working concentrations with RPMI-1640 nutrient medium (Sigma Chemical Co. St Louis, MO) supplemented with 3 mmol/L L-glutamine, 100  $\mu$ g/mL streptomycin, 100 IU/mL penicillin, 10% heat inactivated fetal bovine serum (FBS - Sigma Chemical Co.), and 25 mM HEPES, adjusted to pH 7.2 by bicarbonate solution.

### *Preparation of peripheral blood mononuclear cells (PBMC):*

Three healthy volunteers donated human blood. PBMC were separated from whole heparinized blood by Lymphoprep (Nycomed, Oslo, Norway) gradient centrifugation. Interface cells, washed three times with Haemaccel (aqueous solution supplemented with 145 mM Na<sup>+</sup>, 5.1 mM K<sup>+</sup>, 6.2 mM Ca<sup>2+</sup>, 145 mM Cl<sup>-</sup> and 35 g/L gelatin polymers, pH 7.4), were counted and resuspended in RPMI-1640 nutrient medium with 10% FBS.

### *Treatment of PBMC from normal healthy donors:*

PBMC were seeded at the density of 150,000 cells per well in a nutrient medium only (with 10% FBS), or in a nutrient medium enriched with 5 µg/mL of phytohaemagglutinin (PHA - Welcome Diagnostics, England) in 96-well microtiter plates. Two hours later, investigated compounds were added to the wells, in triplicates, to five final concentrations (within the range of 18.75-300 µM), except to the control wells where a nutrient medium only was added to the cells. Nutrient medium with corresponding concentrations of compounds, but void of cells was used as blank. PBMC's were incubated for 72 hours at 37 °C in humidified atmosphere with 5% CO<sub>2</sub>.

### *Determination of PBMC survival:*

PBMC survival was determined by MTT test according to the method of Mosmann<sup>6</sup> and modified by Ohno and Abe,<sup>7</sup> 72 hours after the drug addition. Briefly, 20 µL of MTT solution (5 mg/mL in phosphate buffered saline) was added to each well. PBMCs were incubated for further four hours at 37 °C in humidified atmosphere with 5% CO<sub>2</sub>. Then, 100 µL of 10% SDS was added to the wells. Absorbance was measured at 570 nm the next day. The cell survival (S%) was measured/quantified using absorbance at 570 nm of a sample with cells grown in the presence of various concentrations of agent was divided with absorbance of control sample (the absorbance of cells grown only in nutrient medium), implying that absorbance of blank was always subtracted from absorbance of a corresponding sample with target cells.

### *Calculation protocols:*

Structures of **1-20** were sketched using ISIS Draw 2.5<sup>8</sup> and imported in VegaZZ 2.2.1<sup>9</sup> molecular modeling package. Based on the NMR spectra of compounds, recorded in solvents having different polarity and HBA/HBD abilities (CDCl<sub>3</sub>, D<sub>2</sub>O, and DMSO-*d*<sub>6</sub>)<sup>2</sup> the prevailing, enolic forms of aryldiketo acids in both neutral and ionised forms were considered during modelling. Initial structures (lowest energy conformations) of **21-24** were obtained by Omega 2.2.1<sup>10</sup> from SMILES notation using MMFF94 force field.<sup>11</sup> Structures of **1-20**, **24** were optimized by semiempirical molecular orbital PM6 method<sup>12</sup> to root mean square (RMS) gradient below 0.01 kcal/mol, by MOPAC2007<sup>13</sup> using implicit solvation (COSMO, setting dielectric constant of the solvent to 78.4 - water). A constraint was imposed in compounds **21-23** on the heavy atoms of the piperazine ring connected to position 7 and C7 of quinolone moiety, and calculations were done under the same condition as for **1-20**. Optimized structures were used as input for ALMOND suite of programs.<sup>14</sup> GRID 22a<sup>15</sup> was used for calculation of MG+2 probe molecular interaction fields with **5**, **8 - 10**, **12**, **15**, **17**, **19**, **21-24**, using grid resolution of 0.5 Å. MOVE directive was kept at default value of 0, so that the movement of flexible parts of molecules was not allowed. The GLUE procedure of the same program was used for calculations of interaction energies between **21** and **1-20**. Conformers of **1-20** monoanions, and **21-24** zwitteranions are built by Omega 2.2.1, using MMFF94s<sup>11</sup> force field, and ROCS 2.3.1<sup>16</sup> was used for superimposition of molecules and similarity analysis. For calculation the 'shape only' directive was set to 'false'. The Accelrys DS Visualizer 2.0 was used for graphical representation of obtained results of similarity analysis. All calculations were done on AMD dual core x64 processor (5 GHz) in Windows or Linux environments. p*K*<sub>a</sub> Prediction of **12** was obtained by MoKa 1.0.9, using prediction library v. 4.3.3.<sup>17</sup>

### *Building ALMOND models:*

Two models were built. First model was obtained using **5**, **8 - 10**, **12**, **15**, **17**, **19** and commercial antibiotics (**21-24**) in their neutral forms-model I; while the second model was built using same molecules

in their ionization states under physiological pH (7.35) - model II. Initial models were built using N1, O, DRY and TIP probes (HBD, HBA, hydrophobic and shape probe, respectively). For both models, the correlograms of the O probe in PLS plots appeared very similar to corresponding ones of N1 probe. For clarity, after first runs, O probe was excluded. 90 nodes were extracted and %weight of field is set to 65 (Model I) and 60 (Model II) for final models (setting of relative weight of field at 50% accounts equal importance of distance and energy product of nodes; our settings gives more weight to the energy product in respect to node distance). TIP cut-off is set to 0.8 Å to avoid close proximity between TIP nodes and nodes of other probes. This resulted with more interpretable final models. Initially, first model (related to molecular forms of compounds) relied on the N1-N1 cross-block that distinguish commercial antibiotics (**21-24**) from the rest. Because of that, this block was excluded and new model was built. For the second model (related to ionized species), the weight assigned to the atomic electrostatic contribution was lowered, setting ALMD directive to 0.6. Models were built by means of partial least square (PLS) using 3 latent variables (LV) for first runs. Final models were derived by 2 LV. Validation of models was done by cross validation using three groups of approximately same size in which the objects were assigned randomly. For the final models “leave two out” and “leave one out” cross validation data were also reported. As all obtained node-node interactions were not relevant for model derivation, the ALMOND built-in fractional factorial design (FFD) was used for variable selections, keeping in models uncertain variables. Final models comprise lower number of variables and should have better predictivity.

## Supporting Results and Discussion

### Cytotoxicity results

**Table 1S.** Cytotoxicity, expressed as IC<sub>50</sub> and IC<sub>90</sub> (concentration that inhibit 50% and 90% growth, respectively), of selected compounds toward healthy human cells PBMC (peripheral blood mononuclear cells) non-stimulated and stimulated for proliferation with phytohaemagglutinin (PHA).

Compound No.	IC <sub>50</sub>		IC <sub>90</sub>	
	PBMC ( $\mu$ M)	PBMC+PHA ( $\mu$ M)	PBMC ( $\mu$ M)	PBMC+PHA ( $\mu$ M)
<b>8</b>	121.4 ( $\pm$ 6)	122.1 ( $\pm$ 1)	265.0 ( $\pm$ 2)	273.0 ( $\pm$ 6)
<b>10</b>	137.4 ( $\pm$ 10)	107.1 ( $\pm$ 2)	265.0 ( $\pm$ 5)	257.0 ( $\pm$ 5)
<b>12</b>	153.5 ( $\pm$ 8)	147.3 ( $\pm$ 11)	>300	296.0 ( $\pm$ 9)
<b>15</b>	>300	>300	>300	>300
<b>17</b>	264.4 ( $\pm$ 10)	247.1 ( $\pm$ 10)	>300	>300
<b>20</b>	>300	>300	>300	>300

## Almond Model

Two models were selected for discussion: model 1 (all molecules were in their neutral form) and model 2 (molecules were in a protonation states that would be adopted at the physiological pH (7.35)).

**Table 2S.** Statistics of PLS model for neutral forms of **5, 8 - 10, 12, 15, 17, 19, 21-24** minimum inhibitory concentrations (MIC) against SA-1199B.

Latent Variables	X Variable Explanation	X Accumulation	SDEC	$r^2$	
<b>1</b>	23.369	23.369	0.328	0.905	
<b>2</b>	15.923	40.292	0.190	0.968	
Latent Variables	SDEP	SDEV	$q^2$ (RG)	$q^2$ (LTO)	$q^2$ (LOO)
<b>1</b>	0.590	0.136	0.692	0.741	0.759
<b>2</b>	0.528	0.138	0.754	0.797	0.812

The statistics:  $r^2$  and  $q^2$  values, standard deviation of error calculation (SDEC) and prediction (SDEP) refer to PLS model obtained after two run of FFD variable selection using the following settings: Max.dim.: 2; 3 random groups; 20 SDEP; recalculated weights; retain uncertain variables; 25% dummies; Comb/Var ratio = 2.5. The same validation method is used to calculate  $q^2$  ( $q^2$  (RG) - Random groups;  $q^2$  (LTO) – Leave two out;  $q^2$  (LOO) – Leave one out) and SDEP.

**Table 3S.** Statistics of PLS model for ionised forms of **5, 8 - 10, 12, 15, 17, 19, 21-24** minimum inhibitory concentrations (MIC) against SA-1199B.

Latent Variables	X Variable Explanation	X Accumulation	SDEC	$r^2$	
<b>1</b>	26.197	26.197	0.288	0.927	
<b>2</b>	10.674	36.872	0.120	0.987	
Latent Variables	SDEP	SDEV	$q^2$ (RG)	$q^2$ (LTO)	$q^2$ (LOO)
<b>1</b>	0.691	0.113	0.579	0.632	0.651
<b>2</b>	0.639	0.113	0.640	0.696	0.723

The statistics:  $r^2$  and  $q^2$  values, standard deviation of error calculation (SDEC) and prediction (SDEP) refer to PLS model obtained after two run of FFD variable selection using the following settings: Max.dim.: 2; 3 random groups; 20 SDEP; recalculated weights; retain uncertain variables; 25% dummies; Comb/Var ratio = 2.5. The same validation method is used to calculate  $q^2$  ( $q^2$  (RG) - Random groups;  $q^2$  (LTO) – Leave two out;  $q^2$  (LOO) – Leave one out) and SDEP.

**Table 4S.** Variables having high impact on the first model related to neutral forms of **5**, **8** -**10**, **12**, **15**, **17**, **19**, and **21** - **24**.

Probe block	Variable N <sup>o</sup>	Distance (Å)	Impact	Regions <sup>a</sup>
DRY-DRY	27	8.64	+	Region of phenyl ring <i>and</i> region of keto-enol double bond for aryldiketo derivatives. Region of C7 substituent alkyl moiety <i>and</i> C2-C3 double bond of <b>21-24</b> .
TIP-TIP	21	6.72	-	Carboxyl HBD-HBA for all compounds.
TIP-TIP	29	9.28	+	Region of carboxyl group <i>and ortho</i> -alkyl substituent for aryldiketo acids or 1-alkyl substituent for <b>21-24</b> .
TIP-TIP	56, 57	17.92-18.24	+	Region of carboxyl group <i>and</i> terminal part of C7 substituent of <b>22-24</b> or <i>para</i> position of <b>12</b> 4'-phenyl.
DRY-N1	24	7.68	+	N1 lobe associated with aroyl carbonyl <i>and</i> distal DRY lobe associated with phenyl ring for aryldiketo acids. For <b>21-24</b> , to DRY probe area contribute nodes of ketopyridone moiety and alkyl substituent in position 1; N1 positioned on distal or proximal N of C7 substituent (carboxyl carbonyl for <b>21</b> ).
DRY-N1	37	11.84	-	DRY on phenyl ring for aryldiketo acids, or alkyl moiety of C7 substituent for <b>21-24</b> . N1 associated with carboxyl carbonyl.
N1-TIP	58	18.88	+	N1 associated with carboxyl carbonyl, TIP associated with most distant part of molecule.

<sup>a</sup> Described as regions of molecules associated with the first *and* the second probe.

**Table 5S.** Variables having high impact on the model for ionized forms of **5, 8-10, 12, 15, 17, 19** and **21-24**.

Probe block	Variable N <sup>o</sup>	Distance (Å)	Impact	Regions <sup>a</sup>
DRY-DRY	24, 25	7.68-8.00	+	Region of ring C connected to aroyl keto <i>and</i> region of C connected to 4 or 5 substituent for aryldiketo derivatives. Region of C7 substituent alkyl moiety <i>and</i> C4'-C10' bond of <b>21-24</b> .
TIP-TIP	17	5.44	-	Mainly carboxylate O-O.
TIP-TIP	31	9.92	+	Region of carboxylate O (or enolate O for dianions) <i>and</i> alkyl substituent (4 or 5 for dianions) for aryldiketo acids or 1-alkyl substituent for <b>21-24</b> .
TIP-TIP	50	16.00	+	Region of carboxylate <i>and</i> 4-substituent of phenyl or terminal part of C7 substituent of <b>22-24</b> .
DRY-N1	22	7.68	+	N1 lobe on aroyl carbonyl <i>and</i> distal DRY lobe of phenyl ring for <b>5, 8-12</b> . For <b>21-24</b> , to DRY probe area contributes nodes of ketopyridone moiety and alkyl substituent in position 1; N1 associated with quinolidine 3-keto group (or distal N of C7 substituent for <b>24</b> ).
DRY-N1	43	13.76	-	DRY on phenyl ring for aryldiketo acids. N1 associated with carboxylate.
N1-TIP	54, 58	17.26 -18.88	+	N1 associated with carboxyl, TIP associated with most distant part of molecule.

<sup>a</sup> Described as regions of molecules associated with the first *and* the second probe.

**Table 6S.** Presence of variables associated with compounds, in the model for neutral forms of **5, 8 - 10, 12, 15, 17, 19** and **21 - 24**.

Compound N <sup>0</sup>	DRY-DRY 27	TIP-TIP 21	TIP-TIP 28	TIP-TIP 58	DRY-N1 8	DRY-N1 25	DRY-N1 37	DRY-TIP 41	N1-TIP 58
<b>5</b>	-	+	+	-	+	+	+	+	-
<b>8</b>	+	+	+	-	+	+	+	+	-
<b>9</b>	-	+	+	-	+	+	+	+	-
<b>10</b>	+	+	+	-	+	+	+	+	-
<b>11</b>	+	+	+	-	+	+	+	+	-
<b>12</b>	-	+	-	+	+	+	+	+	-
<b>15</b>	-	+	+	-	+	+	+	-	-
<b>17</b>	-	+	-	-	+	+	+	+	-
<b>19</b>	-	+	-	-	+	+	+	-	-
<b>21</b>	+	+	+	-	-	+	+	-	-
<b>22</b>	+	+	+	+	-	+	+	+	+
<b>23</b>	+	+	+	+	-	+	+	+	+
<b>24</b>	+	+	+	+	-	+	-	+	+

<sup>a</sup> (DRY-DRY 21) for this compound.

<sup>b</sup> (TIP-TIP 20) for those compounds.

<sup>c</sup> (TIP-TIP 32) for this compound.

**Table 7S.** Presence of variables associated with compounds, in the model for ionized forms of **5, 8 - 10, 12, 15, 17, 19** and **21 - 24**.

Compound N <sup>1e</sup>	DRY-DRY 24	N1-N1 38	TIP-TIP 17	TIP-TIP 31	TIP-TIP 50	DRY-N1 22	DRY-N1 43	N1-TIP 47, 48	N1-TIP 54	N1-TIP 58
<b>5</b>	+	-	+	+	+	+	-	+	-	-
<b>8</b>	+	-	+	+	+	+	-	+	-	-
<b>9</b>	+	-	+	+	-	+	-	+	-	-
<b>10</b>	+	-	+	+	+	+	-	+	-	-
<b>12</b>	-	-	+	+	+	+	+	+	+	-
<b>15</b>	-	-	+	+	-	+	-	+	-	-
<b>17</b>	+	-	+	+	-	+	-	+	-	-
<b>19</b>	-	-	+	-	-	+	-	+	-	-
<b>21</b>	-	-	+	+	+	+	-	+	+	-
<b>22</b>	+	-	+	+	+	+	-	+	+	-
<b>23</b>	+	-	-	+	+	+	-	+	+	+
<b>24</b>	+	+	+	+	+	+	-	-	+	+

**Table 8S.** Observed vs. Calculated log (1/MIC) against SA-1199B for **5, 8 - 10, 12, 15, 17, 19, 21 - 24** in their neutral and ionized forms. MIC is in mol/L.

Compound No.	MIC (M)	Observed Log(1/MIC)	Calculated Log(1/MIC) <sup>a</sup>	Calculated Log(1/MIC) <sup>b</sup>
<b>5</b>	$1.03 \cdot 10^{-3}$	2.987	2.809	3.162
<b>8</b>	$2.32 \cdot 10^{-4}$	3.635	3.729	3.736
<b>9</b>	$2.32 \cdot 10^{-4}$	3.635	3.779	3.605
<b>10</b>	$1.16 \cdot 10^{-4}$	3.936	4.051	3.805
<b>12</b>	$4.77 \cdot 10^{-4}$	3.321	3.223	3.185
<b>15</b>	$2.46 \cdot 10^{-3}$	2.609	2.719	2.579
<b>17</b>	$2.16 \cdot 10^{-3}$	2.666	2.636	2.745
<b>19</b>	$2.26 \cdot 10^{-3}$	2.646	2.434	2.631
<b>21</b>	$1.10 \cdot 10^{-4}$	3.974	4.190	4.148
<b>22</b>	$2.42 \cdot 10^{-5}$	4.616	4.820	4.387
<b>23</b>	$5.53 \cdot 10^{-6}$	5.257	5.336	5.227
<b>24</b>	$6.23 \cdot 10^{-7}$	6.206	5.761	6.279

<sup>a</sup> Calculated for the neutral forms.

<sup>b</sup> Calculated for the ionized forms.

**Table 9S.** GRID MG+2 probe minima for compounds **5, 8 - 10, 12, 15, 17, 19, 21 - 24** in their ionization states under the physiological pH (7.35).

Compound No.	Ionization State	GRID MG+2 probe minima (kcal/mol)
<b>5</b>	HA <sup>-</sup>	-14.100
<b>8</b>	A <sup>2-</sup>	-48.089
<b>9</b>	A <sup>2-</sup>	-46.658
<b>10</b>	A <sup>2-</sup>	-49.620
<b>12</b>	A <sup>2-</sup>	-31.503
<b>15</b>	HA <sup>-</sup>	-10.028
<b>17</b>	HA <sup>-</sup>	-9.420
<b>19</b>	A <sup>2-</sup>	-30.384
<b>21</b>	Zwitterion	-11.609
<b>22</b>	Zwitterion	-11.943
<b>23</b>	Zwitterion	-14.990
<b>24</b>	Zwitterion	-20.170

**Table 10S.** Interaction energies between ADKs and norfloxacin calculated by GLUE without (w/o) and with (w) electrostatic contribution using procedure described previously.<sup>18</sup>

Compound	Interaction energies (kcal/mol)		Potentiation <sup>a</sup>
	w/o	w	
<b>1</b>	-10.5	-15.4	/
<b>2</b>	-11.7	-14.0	/
<b>3</b>	-11.2	-14.7	/
<b>4</b>	-11.6	-14.2	/
<b>5</b>	-9.6	-13.4	/
<b>6</b>	-11.4	-15.1	/
<b>7</b>	-11.5	-15.6	2
<b>8</b>	-10.5	-16.0	/
<b>8</b>	-12.1	-15.4	/
<b>9</b>	-12.6	-14.5	/
<b>10</b>	-11.9	-14.7	/
<b>11</b>	-12.5	-12.3	/
<b>12</b>	-12.3	-15.9	2
<b>13</b>	-12.9	-16.1	/
<b>14</b>	-7.7	-12.9	2
<b>15</b>	-8.0	-12.3	2
<b>16</b>	-8.2	-13.6	/
<b>17</b>	-8.9	-17.2	2
<b>18</b>	-6.0	-7.8	/
<b>19</b>	-8.4	-12.4	/
<b>20</b>	-11.7	-12.9	2

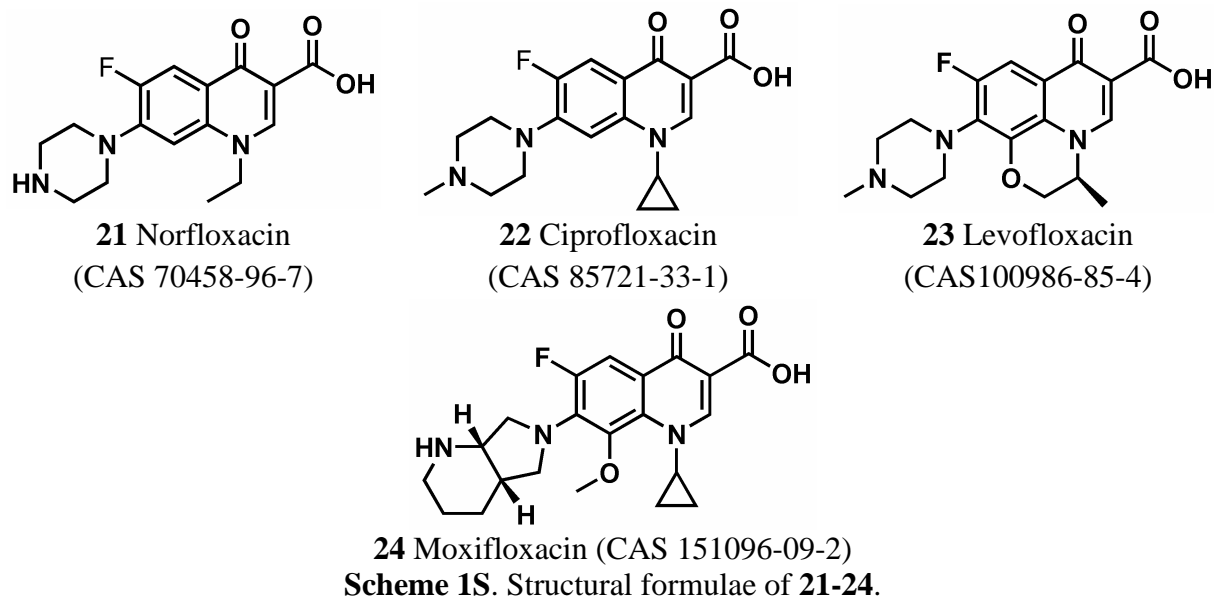
<sup>a</sup> Potentiation was calculated as a ratio between the MIC of **21** in the absence and presence of a compound. The compound was added in the amount of one quarter of its MIC (maximum of 100 µg/ml); / - no change of norfloxacin MIC in presence of ADK.

### *Comparative analysis of ALMOND models related to neutral and ionized forms of molecules*

Briefly, program ALMOND uses alignment independent descriptors derived from GRID molecular interaction fields (MIF). More negative value of GRID MIF for any used probe corresponds to more favorable interaction between a probe (*e.g.* hydrogen bond donor, hydrogen bond acceptor, hydrophobic) and a molecule for which GRID MIF is calculated. By calculating MIFs for different GRID probes around a molecule and extracting most relevant regions one can obtain a fingerprint of a receptor to which small molecule could fit well. These regions show favorable energy of interaction and represent positions where groups of a potential receptor would interact favorably with a ligand. Such MIF pattern can be described as the virtual receptor site (VRS). Each GRIND descriptor consists of two nodes extracted from MIFs and encodes their energy product and spatial distance. GRIND variables represent geometrical relationships between relevant pharmacophore points around studied molecules, which are entirely invariable to position of molecule(s) in space and alignment of molecules. Derivation of GRIND descriptors includes next steps: (i) computing a set of MIF around studied molecules, (ii) filtering the MIF, to extract the most relevant regions that define the VRS, and (iii) encoding the VRS into the GRIND variables. GRIND variables can be used for comparison of molecules and their classification within sets of structurally diverse entities, and ALMOND program use principal component analysis (PCA) for this type of analysis.

An independent variable (such is biological activity of a certain type) can be correlated to GRIND descriptors (as dependent variables) obtained on a set of molecules by partial least square analysis (PLS). Most intensive bars in the PLS plots (Panels I and II) have the highest impact on a model. Bars having positive values on y scale represent variables positively correlated with activity, while those having negative values on y scale are negatively correlated with activity. Within the each block (auto- or cross-correlograms, that correspond to pairs of nodes of a same or a different probe, respectively) variables are arranged from left to right on the x scale of the plot according to ascending distance between their nodes. In addition to the spatial arrangement of molecules and nodes encoded in GRIND variables, each node of each variable exert specific energy of interaction with a target molecule. Therefore, the strength of

interaction between respective GRID probe in particular nodes and molecules are accounted in addition to spatial positions of VRS regions. More detail information on the method can be found in original references.<sup>14</sup>



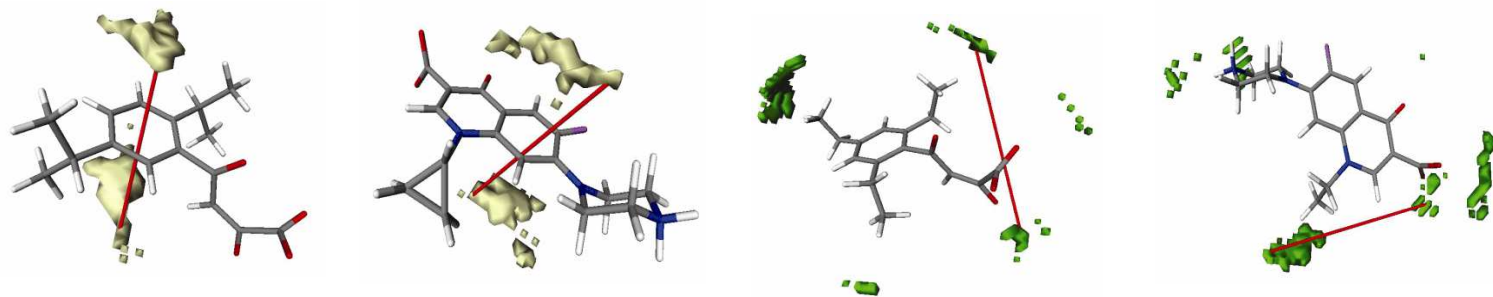
Two ALMOND models were built, first related to molecules in their neutral forms, and the second related to molecules in their ionized forms, at physiological pH. Conformations of molecules used in both models were obtained by geometry minimization on a semiempirical level of calculation using an implicit solvent model, and should represent prevalent conformations in solution.

Despite the fact that ionized forms had significantly different conformations from their corresponding neutral forms and the ALMOND probes exhibited different interactions (mainly in intensities and not positions), the majority of variables having high impact in both models were very comparable. Both models readily detected structural similarity between moieties of studied aryldiketo acids (**5**, **8-10**, **12**, **15**, **17**, **19**) and fluoroquinolone antibiotics (**21-24**) by both positions of nodes around molecules and their interaction energies (IE). All similar regions were positively correlated with potency.

Graphical presentation of PLS coefficient plots and variables associated with compounds, are given in Panels I and II for models that correspond to ionized and neutral form of compounds, respectively. For illustration, important variables associated with compounds are also given in the Panels I and II.

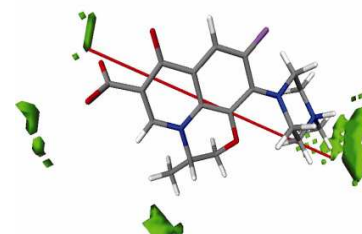
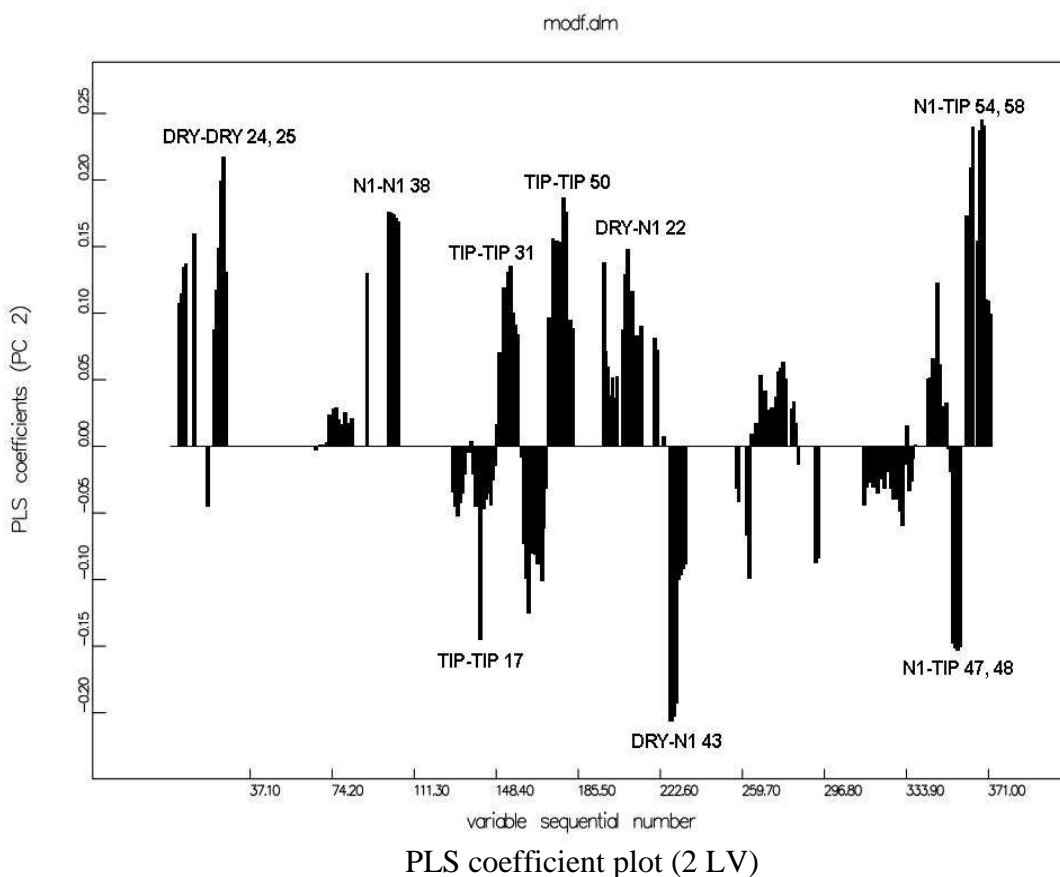
Subsequent analysis emphasizes only similarity between studied aryldiketo acids (**5**, **8-10**, **12**, **15**, **17**, **19**) and fluoroquinolone antibiotics (**21-24**) and does not offer full interpretation of the models.

Panel I: Model for ionized forms of compounds.

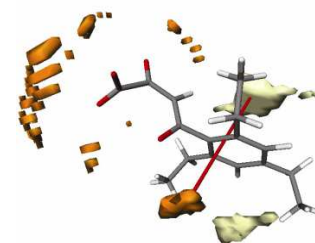


Variable DRY-DRY 25 for **9** (left) and **22** (right)

Variable TIP-TIP 31 for **10** (left) and **22** (right)

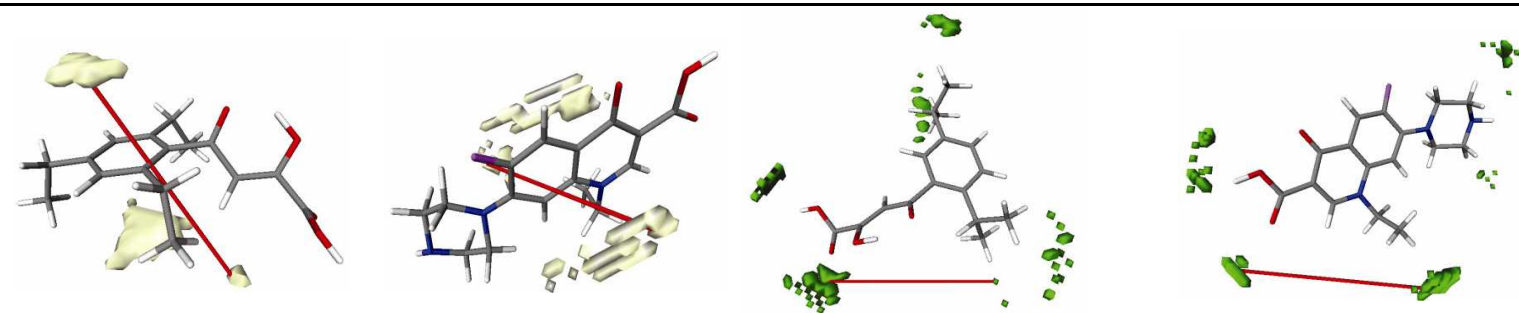


Variable TIP-TIP 50 for **23**



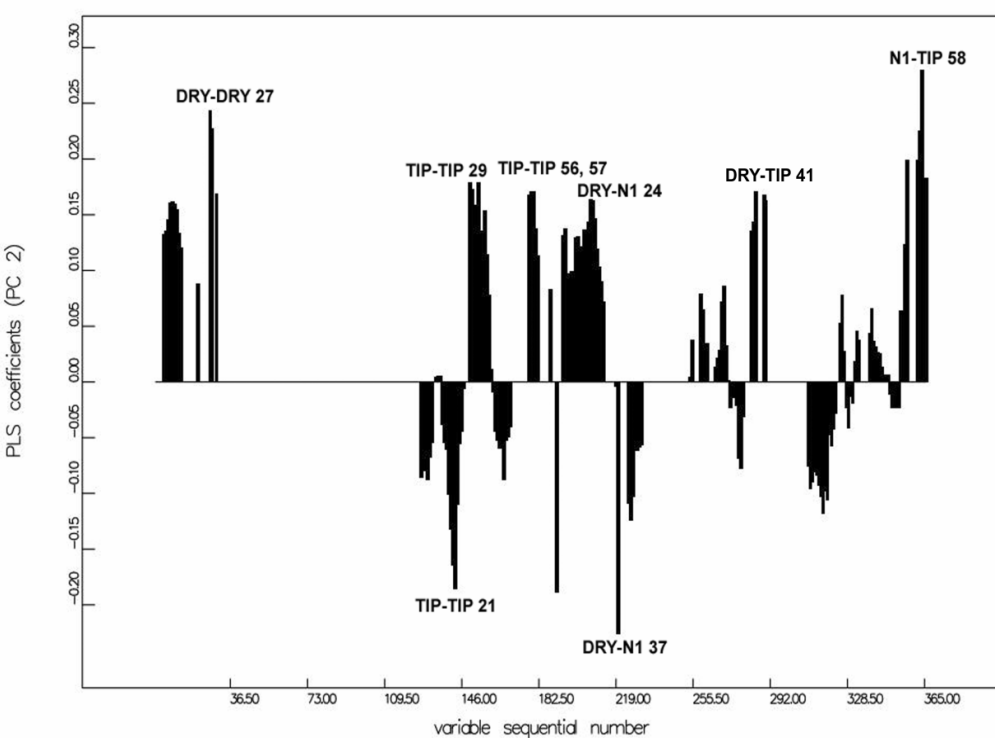
Variable DRY-N1 22 for **10** (up) and **22** (down)

Panel II: Model for neutral forms of compounds.

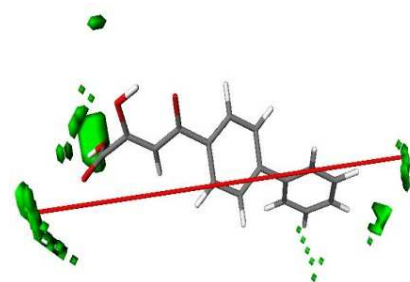


Variable DRY-DRY 27 for **8** (left) and **21** (right)

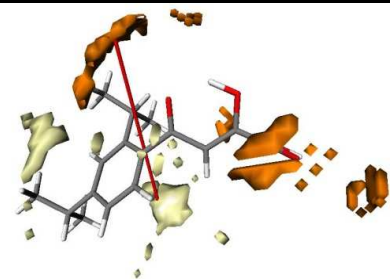
Variable TIP-TIP 31 for **10** (left) and **22** (right)



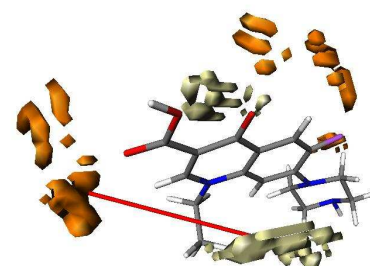
PLS coefficient plot (2 LV)



TIP-TIP 56 for **12**



Variable DRY-N1 24 for **10** (up) and **21** (down)



Similarity between 4-phenyl-4-oxo-2-butenic moiety and quinolone core of **21-24** was observed by variable DRY-DRY 27 of the first model, related to neutral form of the studied compounds, and variables DRY-DRY 24 and 25 of the model related to ionized compounds. One node of these variables was always positioned proximal to phenyl rings of aryldiketo acid or of the quinolone core, while other was positioned in the proximity to 4-oxo-2-butenic moiety or the pyridone C=C double bonds.

The spatial arrangement between the carboxyl group and the *ortho*-alkyl substituent of aryldiketo acids (**8-10**) was compared to the spatial arrangement of the 3-carboxyl group of the quinolone core and alkyl substituent in its position 1, as given by variable TIP-TIP 29 (31 for the model related to ionized form of molecules).

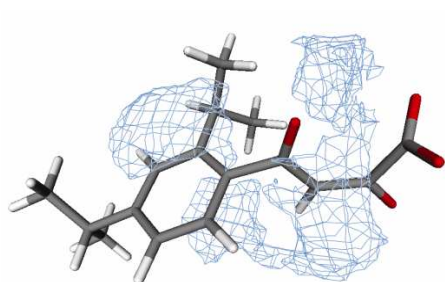
Variables TIP-TIP 56 or 57 (50 for the model related to ionized form of molecules), roughly corresponded to the "length" of molecules, since one node of a variable was associated with carboxyl moieties and the second node was associated with the most distal part of a molecule. It should be noted that this variable only had non zero value for compound **12** in the first model, while the same variable had significant intensity for the majority of the most potent aryldiketo acids in the model related to ionized form of molecules (Tables S6 and S7). This emphasized that all studied molecules were mutually more similar in physiological (di)anion form, than in their corresponding neutral form.

Additional similarity between potential pharmacophoric points of aryldiketo acids and fluoroquinolone molecules was given by the variable DRY-N1 24 (22 for the model related to ionized form of molecules). For aryldiketo acids, N1 node was associated with the aroyl keto group and the DRY node was associated with the interaction region of the probe with the phenyl ring. For fluoroquinolone molecules, the N1 node was associated with the keto group in position 3 (proximal tertiary N of C7 substituent for **24**) and the DRY node was situated within area of the aromatic quinolone core and the alkyl substituent in its position 1.

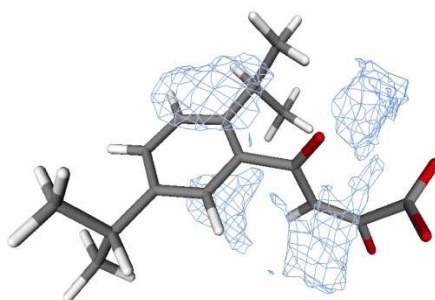
The distinction between the more potent fluoroquinolone molecules (**21-24**) and the aryldiketo acids was given by variable N1-TIP 58 which had high intensity only for fluoroquinolone molecules.

Considering fluoroquinolone antibiotics pharmacophore pattern, it could be concluded that the most potent aryldiketo acids (**8-10**) from the studied set matched well with the quinolone core and the substituents in their R1, R3, and R4 positions, as well as the length of molecules for bulkier compound (**12**). Along with the quinolone C7 substituent, these are the most important moieties of fluoroquinolone responsible for antibacterial activity.

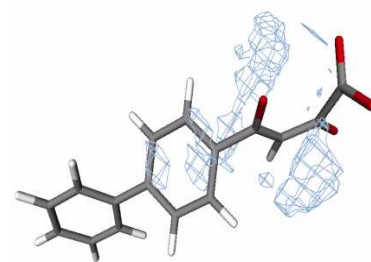
**Figure 1S.** MG+2 GRID probe isocountour levels for **8**, **9**, **12**, **22** and **23**, in their ionized forms on physiological pH (7.35).



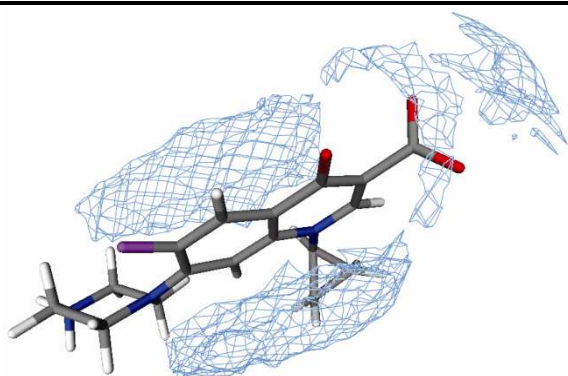
GRID MG+2 probe isocontour level on  $-22.2$  kcal/mol for  $A^{2-}$  form of **8**



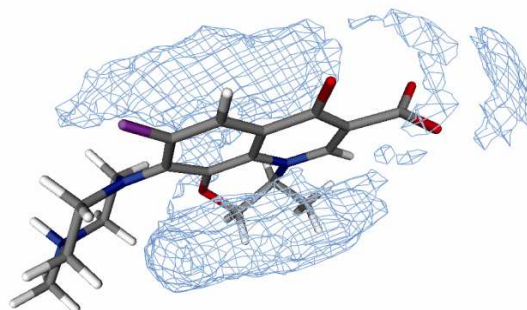
GRID MG+2 probe isocontour level on  $-25$  kcal/mol for  $A^{2-}$  form of **9**



GRID MG+2 probe isocontour level on  $-15.4$  kcal/mol for  $A^{2-}$  form of **12**



GRID MG+2 probe isocontour level on  $-4.3$  kcal/mol for zwitteranion form of **22**



GRID MG+2 probe isocontour level on  $-4.4$  kcal/mol for zwitteranion form of **23**

## References

- [1] Verbić, T. Ž.; Drakulić, B. J.; Zloh, M. F.; Pecelj, J. R.; Popović, G. V.; Juranić, I. O. *J. Serb. Chem. Soc.* **2007**, 72 (12), 1201-1216.
- [2] Verbić, T. Ž.; Drakulić, B. J.; Zloh, M.; Juranić, I. O. *Lett. Org. Chem.* **2008**, 5 (8), 692-699.
- [3] Ross, J. I., Farrell, A. M., Eady, E. A., Cove J. H., Cunliffe, W. J. *J. Antimicrob. Chemother.* **1989**, 24, 851–862.
- [4] Gibbons, S., Udo, E. E. *Phytother. Res.* **2000**, 14, 139–140.
- [5] Kaatz, G. W., Seo, S. M., Ruble, C. A. *Antimicrob. Agents Chemother.* **1993**, 37, 1086–1094.
- [6] Mosmann, T. *J. Immunol Meth.* 1983, 65, 55-63.
- [7] Ohno, M, Abe, T. *J. Immunol. Meth.* **1991**, 145, 199–203.
- [8] MDL ISIS Draw 2.5, MDL information System Inc. 2002
- [9] Pedretti, A., Villa, L., Vistoli, G. *J. Comput. Aid. Mol. Des.* **2004**, 18, 167-173,  
<http://www.ddl.unimi.it>
- [10] Boström, J.; Greenwood, J. R.; Gottfries, J. *J. Mol. Graph. Mod.* **2003**, 21, 449-462;  
<http://www.eyesopen.com/products/applications/omega.html>
- [11] Halgren, T. A. *J. Comp. Chem.* **1999**, 20, 730-748.
- [12] Stewart, J. J. P. *J. Mol. Mod.* **2007**, 13, 1173-1213.
- [13] Stewart, J. J. P. *J. Comput. Aid. Mol. Des.* **1990**, 4, 1-105; b) MOPAC 2007 James J. P. Stewart, Stewart Computational Chemistry, Colorado Springs, CO, USA, 2007; <http://openmopac.net/>
- [14] a) Pastor, M., Cruciani, G., McLay, I., Pickett, S., Clementi, S. *J. Med. Chem.* **2000**, 43, 3233-3243;  
b) Fontaine, F., Pastor, M., Sanz, F. *J. Med. Chem.* **2004**, 47, 2805-2815; c) ALMOND v. 3.3.0, Molecular Discovery Ltd. <http://www.moldiscovery.com>
- [15] Goodford, P. J. *J. Med. Chem.*, **1985**, 28, 849-857. GRID v.22 Molecular Discovery Ltd.,  
<http://www.moldiscovery.com>
- [16] Mills, J. E. J.; Dean, P. M. *J. Comput-Aided Mol. Des.* **1996**, 10, 607-622;  
<http://www.eyesopen.com/products/applications/rocs.html>
- [17] Milletti, F.; Storchi, L.; Sforza, G; Cruciani, G. *J. Chem. Inf. Mod.*, **2007**, 47(6), 2172-2181; MoKa 1.0.9, [www.moldiscovery.com](http://www.moldiscovery.com)

[18] Zloh, M., Kaatz, G.W., Gibbons, S. *Bioorg. Med. Chem. Lett.* **2004**, *14*, 881-885.